Decoding the Human Brain during Intelligence Testing

Jonas A. Thiele[a], Joshua Faskowitz[b], Olaf Sporns[b], Adam Chuderski[c], Rex Jung[d], Kirsten Hilger[a]*

[a] Department of Psychology I, Würzburg University, Marcusstr. 9-11, Würzburg D-97070, Germany

[b] Department of Psychological and Brain Sciences, Indiana University, 1101 E. 10th St., Bloomington, IN 47405-7007, USA

[c] Centre for Cognitive Science, Jagiellonian University, Ingardena 3, 30-060 Krakow, Poland

[d] The University of New Mexico, Department of Psychology, Logan Hall MSC03-2220, 1 University of New Mexico, Albuquerque, NM 87131-0001, USA

E-mail address and ORCID:

Jonas A. Thiele: jonas.thiele@uni-wuerzburg.de, 0000-0003-2702-9690

Adam Chuderski: adam.chuderski@uj.edu.pl, 0000-0001-6198-674

Olaf Sporns: osporns@indiana.edu, 0000-0001-7265-4036

Rex Jung: rex.jung@runbox.com, 0000-0003-3718-0597

Kirsten Hilger: kirsten.hilger@uni-wuerzburg.de, 0000-0003-3940-5884

* Corresponding author:

Kirsten Hilger

Department of Psychology I

Marcusstr. 9-11

D-97070 Würzburg

E-mail address: kirsten.hilger@uni-wuerzburg.de **Phone:** +49 931 31-81141

Abstract

Understanding the mechanisms of the human brain enabling complex cognition is a major objective of neuroscientific research. Studies employing functional magnetic resonance imaging (fMRI) and electroencephalography (EEG) identified increased activation in specific brain regions during different cognitive states. However, the neural processes during the performance of an intelligence test remains largely unknown. This study considers intelligence as a whole-brain network phenomenon and investigates how the connectedness of specific brain regions contributes to performance on the Raven Progressive Matrices (RAPM), a well-established intelligence test. Connectedness was characterized with graph-theoretical measures based on functional connectivity derived from fMRI BOLD (*N*=67) and EEG theta-band (*N*=128) activity. The results reveal that the extent to which specific frontal and parietal regions are connected to other brain systems during intelligence testing relates to individual test performance. These regions may act as controllers, enabling flexible and efficient switches between cognitive states required to excel in intelligence tests.

Keywords: Intelligence, Raven's Advanced Matrices (RAPM), EEG, fMRI, Functional Connectivity, Connector Hubs.

1 Introduction

Intelligence captures a person's individual level of general cognitive ability. It predicts important life outcomes, including academic achievement, health, and longevity (Calvin et al., 2011; Deary, 2012). For more than a hundred years, research has been seeking its biological bases (Spearman, 1904; Haier, 2017), mostly focusing on the central nervous system (Galton, 1883). Across the last decade, numerous associations between individual intelligence scores and characteristics of brain structure and function have been identified with techniques like functional magnetic-resonance imaging (fMRI) and electroencephalography (EEG) (Hilger et al., 2022).

The Parieto-Frontal Integration Theory (P-FIT) is one of the most influential theories regarding the neural basis of intelligence. It proposes that both structural and functional characteristics of circumscribed brain regions, particularly the communication between frontal and parietal brain regions, is crucial to differences in intelligence (Basten et al., 2015; Jung & Haier, 2007). More recent proposals expanded this model, including the Brain Connectivity Model (BCM, Hilger & Sporns, 2021) and the Network Neuroscience Theory of Intelligence (NNT, Barbey, 2018). While the BCM presents an extensive summary of empirical studies but lacks mechanistic hypotheses, the NNT proposes the flexibility to transition between different brain network states as critical to explain variation in intelligence (Anderson & Barbey, 2023; Barbey, 2018). However, direct empirical evidence supporting the NNT is limited (Girn et al., 2019).

In general, network flexibility might be based on functionally well-connected brain regions (connector hubs; Guimerà & Amaral, 2005) orchestrating changes of activity patterns (network states) to meet external demands (Barbey, 2018, Cole et al. 2013). Previous fMRI research supports the critical role of network efficiency and flexibility for human behavior

and thought (Safron et al., 2022). In resting-state functional connectivity studies, variations in the efficient connectedness of hub regions (Cole et al., 2015; Hilger et al., 2017) as well as the stability and flexibility of brain network organization over time were identified as significant correlates of intelligence (Hilger et al., 2020; Ng et al., 2024; Sassenberg et al., 2024; Saxe et al., 2018). Further, studies assessing functional connectivity during task demands suggest that adapting brain networks fluidly (Shine et al., 2019) and efficiently (Braun et al., 2015; Schultz & Cole, 2016; Thiele et al., 2022) to different demands, supports intelligence-related cognitive processing. Finally, EEG studies provide complementing insights at higher temporal resolution and support the association between functional brain network organization and intelligence. While the early pioneer study by Langer et al. (2012) demonstrated efficiency-related graph parameters (path length) as related to intelligence during resting states, more recent work revealed associations between intelligence and the degree of connectivity in midfrontal theta, reflecting the efficiency of long-range connections during a cognitive task requiring processing speed (Schubert et al., 2021). Notably, most of these previous flexibility-focused studies were based on functional brain connectivity recorded during resting state or during tasks requiring little cognitive effort. Although tasks with increasing difficulty have been considered (Hearne et al., 2017; Sripada et al., 2020), research on tasks directly linked to intelligence-related cognitive processing (Schubert et al., 2021; Soreq et al., 2021) remains rare (Thiele et al., 2022, 2024). Studies during performing intelligence tests - such as the Raven Progressive Matrices (RPM) - might provide more insight.

Using fMRI recorded during RPM, early studies observed associations between individual differences in intelligence and variations in brain activity in frontal and (posterior) parietal cortex (Ebisch et al., 2012; Lee et al., 2006; Perfetti et al., 2009), in the insula (Ebisch et al., 2012) as well as in regions of the default mode network (DMN, Zurrin et al., 2024). EEG recorded during RPM demonstrated associations between intelligence and brain activity

(power) in multiple frequency bands (Ociepka et al., 2023), relations between intelligence scores and differences in delta-gamma (Gągol et al., 2018) and theta-gamma cross-frequency coupling (Pahor & Jaušovec, 2014), and revealed connectivity strength (between the left precentral gyrus and left dorsal cingulate) as being related to intelligence (Caudle et al., 2023).

Notably, not only connectivity strength alone but rather the ability of brain regions to interact (Rubinov & Sporns, 2010) and to induce changes in brain network states that enable efficient adaption to cognitive demands (Barbey, 2018) might inform about individual's cognitive potential. This ability is reflected in the centrality with which brain regions are embedded within the brain's network (Power et al., 2013; Rubinov & Sporns, 2010). Accordingly, the centrality of specific brain regions, measured by the graph-theoretical measures degree and participation coefficient have been related to individual intelligence in studies using theta-band EEG (e.g., Schubert et al., 2021) and fMRI (e.g., Hilger et al., 2017; Thiele et al., 2024). However, whether the centrality of brain regions during an intelligence test is related to individual differences in intelligence, has not yet been investigated – neither with fMRI nor with EEG. Also, it remains an open question, if the overall connectedness of a brain region (degree) or its intermodular connectedness (the diversity of connection of a brain region to different functional brain systems/modules, reflected by the participation coefficient) can explain individual performance in intelligence tests. This study addresses these questions by using fMRI data from 67 participants and EEG data from 128 participants assessed during Raven's Progressive Matrices (RPM).

2 Methods

We used neuroscientific data sets from two independent laboratories; the first to address the question from a neuroimaging perspective and to identify relevant brain regions, the second to

consider the added effects of electrophysiological measures. The first sample comprises fMRI data from 85 participants of one resting-state run and three runs recorded during solving items from Raven's Standard Progressive Matrices (RSPM) as well as items from Raven's Advanced Progressive Matrices (RAPM; Raven, 1990; Raven et al., 1998), including data previously published by Vakhtin et al. (2014). These data were recorded under supervision of Rex Jung (University of New Mexico) at the Mind Research Network (MRN), Albuquerque, NM. The second data set comprises EEG data of 161 participants recorded during resting state and during Raven's Advanced Progressive Matrices (Raven et al., 1998) with 36 items. Data was provided by the research group of Adam Chuderski (Centre for Cognitive Science, Jagiellonian University in Krakow), including data published by Ociepka et al. (2023). Note that, due to the mix of RSPM and RAPM items in the first sample, for both samples, items are referred to collectively as RPM items in the subsequent text. Each RPM item presents a three-by-three matrix with eight elements of geometric shapes and one missing element. This missing element must be solved from the other elements that are linked to each other by logical rules.

2.1 Sample 1

Sample 1 included 85 participants (34 females, age range: 18-29 years, *M*: 22.35; *SD*: 3.14) that were screened and excluded if they reported past major head injuries, psychiatric or neurological disorders, substance abuse, or consumption of any psychoactive medications. Informed consent was obtained from all participants. The study and consent form were approved by the UNM Institutional Review Board, and all procedures were implemented in accordance with the Declaration of Helsinki.

2.1.1 Stimuli and experimental procedure

Each RPM run included 10 pseudo-randomly sampled items. Each item was presented for a maximum time of 15 seconds without showing the solution possibilities. Participants were

instructed to push a button once they solved the item. After pushing the button or 15 seconds had passed a solution set appeared on the screen, and the correct solution was selected out of four possible solutions by pressing one of four buttons corresponding to the index and middle finger of either hand. Between each item, there was a period of 12 to 15 seconds during which a fixation cross was shown.

2.1.2 Functional MRI data acquisition

Functional MRI data were acquired using a 3T Siemens Trio scanner. Specifically, T2*-weighted functional images were obtained with a gradient-echo echo planar imaging sequence (echo time: 29ms, repetition time: 2s, 75° flip angle, 3.5 mm slice thickness, 30% distance factor, 240 mm field of view, voxel size: 3.8 mm × 3.8 mm × 3.5 mm). Resting-state runs lasted 5 minutes and 16 seconds, whereas RPM runs had a length of 5 minutes and 50 seconds.

2.1.3 Functional MRI preprocessing

Basic preprocessing of fMRI data was performed using FMRIPREP (Esteban et al., 2018, 2019) and is descibed in detail in the Supplementary Information. Briefly, preprocessing in FMRIPREP included intensity non-uniformity correction (Tustison et al., 2010), skull-stripping of each T1w volume as well as surface reconstruction (Dale et al., 1999) and spatial normalization to the ICBM 152 Nonlinear Asymmetrical template (Fonov et al., 2009). Functional data were slice time (Cox & Hyde, 1997) and motion corrected (Jenkinson et al., 2002) which was followed by co-registration to the corresponding T1w using boundary-based registration (Greve & Fischl, 2009). Further preprocessing steps comprised high pass filtering with 0.008 Hz and a nuisance regression strategy according to Parkes et al. (Parkes et al., 2018; pipeline no. 7) including 24 head motion regressors, and 10 components (aCompCor, five white matter and five cerebral fluid) from a principal component analysis (PCA) to putative nuisance signals (Muschelli et al., 2014). For data recorded during the RPM, basis-set

task regressors (Cole et al., 2019) were applied simultaneously with the nuisance regressors to remove task-evoked neural activity, as task activation has been shown to produce systematic inflation of task functional connectivity estimates (Cole et al., 2019). Finally, time series of nuisance-regressed blood oxygen-level dependent (BOLD) activity were extracted from 200 nodes covering the entire cortex (Schaefer et al. 2018). Participants were excluded, if the mean framewise displacement (FD) exceeded 0.5 mm, any spikes above 5 mm were detected or if problem-solving times in the RPM runs (see section *Statistical analysis*) were much shorter than expected. The final sample consisted of 67 participants with an age range of 18-29 years (mean age: 22.91 years, age SD: 3.19 years) including 26 females.

2.1.4 Functional MRI-based functional brain connectivity

Functional connectivity between all 200 cortical nodes was estimated as Pearson correlation between z-standardized BOLD signal time series of a) the resting-state run, and b) the three concatenated RPM runs. Note that for the RPM runs, only those time-points were selected during which the RPM items were presented. Those periods depended on the individual time a participant took to solve an item. For this reason, time points were filtered by taking the *n* highest points of the individual's expected hemodynamic response, with *n* equals the duration of the presentation of the respective item. Afterward, functional connectivity matrices were Fisher-z-transformed.

2.2 Sample 2

Sample 2 included 161 right-handed participants (77 females, age range: 18-40 years, *M*: 23.60, *SD*: 4.28). All participants had normal or corrected-to-normal vision, and no history of neurological problems. The study was approved by the local ethics board, informed consent was obtained from each participant, and all procedures were implemented in accordance with the Declaration of Helsinki.

2.2.1 Stimuli and experimental procedure

The order of the RPM items was randomized for each participant. Each item was presented on a screen for 30 seconds without the solution possibilities. Afterward, the solution possibilities were shown, and the correct solution had to be selected within a time window of 20 seconds. Only EEG data recorded during the time in which RPM items but not solution possibilities were displayed was used for further analysis.

2.2.2 EEG data acquisition

Data were recorded in a sound-shielded cabin under supervision of an experimenter. First, 360 seconds of resting-state EEG were acquired followed by the RPM task. EEG was obtained using the Biosemi Active Two system with 64 Ag/AgCl scalp electrodes arranged in accordance with the 10-20 layout. Four further electrodes were placed above and below the left eye and in the external canthi of both eyes to capture vertical and horizontal electrooculograms (EOGs). Voltage values were referenced to zero (quantified relative to the driven right leg and common mode sense loop) and digitized at a sampling rate of 256 Hz.

2.2.3 EEG preprocessing

Preprocessing was done in MATLAB using EEGLAB (v2023.1, Delorme & Makeig, 2004). EEG data were re-referenced to average reference including all 64 scalp electrodes. Next, a high-pass filter (1 Hz) and a notch filter (49.5-50.5 Hz) were applied, and ocular artifacts were corrected using the recursive least squares method (He et al., 2004) as implemented in the EEGLAB plug-in ARR (Gomez-Herrero et al., 2006). Following, resting-state data were segmented into 10 second and RPM data into 30 second epochs. Channels exceeding amplitudes of ±160 µV were interpolated and epochs were removed if more than half the channels exceeded this threshold using the EEG-Plugin TBT (Ben-Shachar, 2018). Further preprocessing steps included the detection and removal of epochs of idle activity in the RPM data, as participants had a fixed time window of 30 seconds after which they had to indicate their response, but it was not registered how long each participant actually worked on solving

the item. To this aim, occipital alpha power (high alpha indicating low cognitive effort) was computed over time for each trial using FieldTrip (Oostenveld et al., 2011). Specifically, alpha power was calculated using multitaper time-frequency with Hanning windows for the frequency range of 9 to 11 Hz. Following, EEG data were segmented into 2 second epochs and epochs were removed if occipital alpha power exceeded a threshold in more than 10% of the time-points. The threshold was visually adjusted and fixed to the mean of the lowest 30% of occipital alpha power plus two standard deviations of whole-trial occipital alpha power for each individual trial. Participants were excluded if demographic information (required as control variables) was missing (age, sex) or when fewer artifact-free RPM epochs than resting-state epochs remained for analysis (see section *Statistical analysis*). This resulted in 128 participants (64 females, age range: 18-40 years, *M*: 23.66, *SD*: 4.34;) for sample 2.

2.2.4 EEG-based functional brain connectivity

Functional connectivity between all 64 EEG channels (serving as network nodes) was computed for resting state and RPM separately (both segmented into 2 second epochs) in a frequency range of 4-7 Hz (theta-band) with a resolution of 0.5 Hz (Schubert et al., 2020) using the debiased weighted Phase Lag Index (dwPLI) implemented with FieldTrip (Gil Ávila et al., 2023; Oostenveld et al., 2011).

2.3 Graph-theoretical measures

Two graph-theoretical centrality measures, degree and participation coefficient, were calculated for each node using the MATLAB-based Brain Connectivity Toolbox (BCT; Rubinov & Sporns, 2010) to capture a) the overall connectedness of a brain region within the network and b) this region's involvement in connections linking different brain systems (diversity of intermodular connectedness). Both measures were determined on proportionally thresholded (50%) functional connectivity matrices. For testing whether the threshold critically affects results, all analyses were repeated with proportional thresholds of 40% and

60%. For the EEG analysis, both measures were calculated for each frequency in the theta-range (4-7 Hz) and each epoch and then averaged across all epochs and theta-range frequencies). To best assess RPM-related cognitive processing, individuals' resting-state measures were subtracted from the RPM measures for both EEG and fMRI analyses.

2.3.1. Overall connectedness: Degree

The degree *k* of a given node *i* expresses how strongly this node is connected to all other nodes in the network and is calculated as sum of all weights (strengths) from adjacent connections, as follows:

$$k_i = \sum_{j \varepsilon N} w_{ij}$$

where w_{ij} represents the functional connectivity strength between node *i* and node *j*, and *N* is the number of nodes in the network (Rubinov & Sporns, 2010).

2.3.2 Intermodular connectedness: Participation coefficient

The participation coefficient *y* of a node *i* assesses the diversity of its intermodular connections and is calculated based on modules within the functional network, as follows:

$$y_i = 1 - \sum_{m \varepsilon M} \left(\frac{k_i(m)}{k_i} \right)^2$$

where *M* is the set of modules (clusters of nodes), k_i is the node's degree (see above), and $k_i(m)$ is the sum of strengths of connections between *i* and all nodes in module *m* (Rubinov & Sporns, 2010). For fMRI, nodes were assigned to the established fMRI-based partition of Yeo et al. (2011) including seven functional brain networks that served as network modules. For EEG, modules were estimated with the Louvain algorithm (Blondel et al., 2008; Reichardt & Bornholdt, 2006; Ronhovde & Nussinov, 2009; Rubinov & Sporns, 2011; Sun et al., 2009) on the group-average resting-state functional connectivity matrix. Herein, a spatial resolution level of $\gamma = 2$ was used, as it resulted in a biologically meaningful number of brain

modules, i.e., between 5 to 10. The Louvain algorithm was repeated 100 times, and a consensus community affiliation (module assignment) was determined across all runs.

2.4 Statistical analysis

Intelligence was operationalized as sum score of the RPM, defined as the number of correctly solved items. Associations between brain measures and intelligence were determined as partial Spearman correlations controlled for age, sex (EEG and fMRI analyses), mean frame-wise displacement (fMRI analysis), and for the number of removed epochs due to artifacts and high occipital alpha (EEG analysis). Statistical significance was accepted for $p < .05$. *P*-values were corrected via the false discovery rate (FDR, number of nodes). Note that because of the exploratory character of this study (high number of brain regions/electrodes included) and due to the hypotheses-generating purpose of our study, we also report effects without correction for multiple comparisons, indicated as *p*, in addition to corrected *p*-values, indicated as *p(adj)*.

For most, but not all, participants, the RPM data comprised more time frames/epochs than the resting-state data. Therefore, to prevent statistical artifacts due to different data lengths, participants with fewer RPM time frames/epochs than resting-state frames/epochs were excluded. Further, the RPM data was shortened to fit the length of the resting-state trials (158 frames for fMRI and 180 epochs with 2 second lengths for EEG). Shortening the data was done by randomly selecting time frames/epochs to be excluded and was repeated 100 times. Following, centrality measures were averaged across these 100 iterations.

2.5 Data and Code Availability

All data and analyses code has been made freely available. EEG data: https://osf.io/kv2sx (resting state), https://osf.io/htrsg (RPM), fMRI data and all analyses code: https://github.com/jonasAthiele/connectors_intelligence.

3 Results

3.1 Intelligence

In both samples, RPM sum scores were approximately normally distributed (*Supplement* Fig. S1). In Sample 1, scores ranged from 9.6 to 30 with a mean of 21.65, a standard deviation of 4.48 and they were not significantly correlated with age (*rho* = .16, *p* = .197), sex (*rho* = -.19, *p* = .114) or framewise displacement (*rho* = -.12, *p* = .354). In Sample 2, RPM scores ranged between 3 and 31 with a mean of 20.48 and a standard deviation of 5.17. The scores were significantly negatively correlated with age (*rho* = -.22, *p* = .013), while no significant correlation with sex (*rho* = .05, *p* = .583) or the number of removed epochs (*rho* = -.17, *p* = .063) was observed. Note that as in Sample 1 only 30 items had to be solved, whereas in Sample 2 the test consisted of 36 items, the scores listed above for Sample 1 are the original scores multiplied by the factor 36/30, thus allowing for better comparison between both samples.

3.2 Functional MRI-based brain network centrality

Group-average functional connectivity matrices of the resting state, the RPM test as well as the difference between RPM and resting-state functional connectivity are shown in *Supplement* Figs S2-S4. Replicating previous studies that compared resting-state functional connectivity with functional connectivity obtained during other tasks (e.g., Schulz and Cole, 2016), task performance led to a decrease in connectivity in primary sensory unimodal areas, while increased connectivity was observed in multimodal associative regions, as compared to resting state. Descriptively, this increase was strongest for connectivity between the default mode network and the ventral attention network.

Group-average brain maps of both graph-theoretical centrality measures, i.e., degree and participation coefficient, obtained during resting state and during RPM as well as their rest-task difference are displayed in Figures 1 and 2. During RPM performance, degree was

descriptively higher in bilateral regions of the medial and dorsolateral prefrontal cortex, in wide-spread regions of the medial parietal cortex as well as in bilateral areas around the temporo-parietal junction areas (TPJ), while it was slightly lower in some visual, temporal and motor regions compared to resting state. Regarding the participation coefficient, a similar but more localized pattern was observed when transitioning from resting state to RPM with increases in the dorsolateral, dorsomedial, and ventromedial prefrontal cortices, and in bilateral TPJs including parts of the inferior partial lobules (IPL) and the superior temporal sulci (STS).

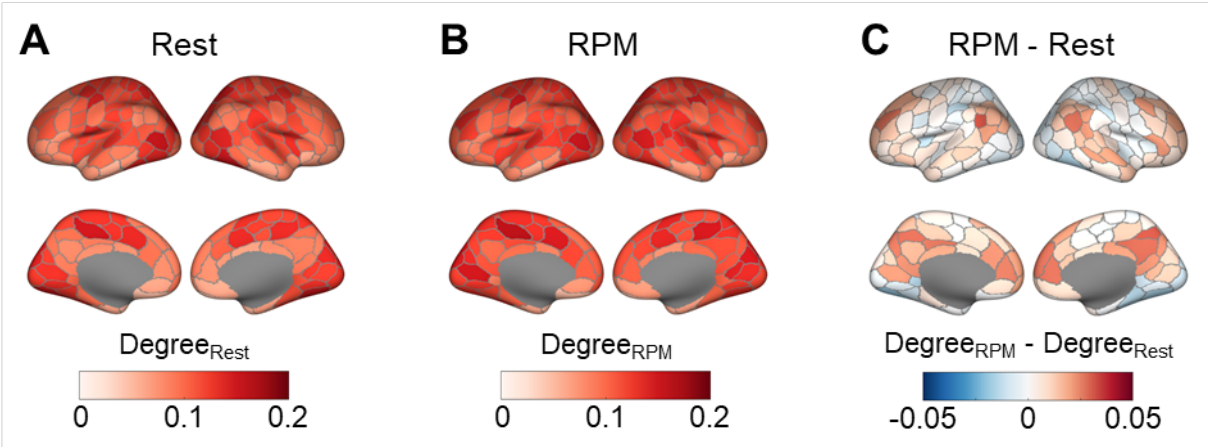

Figure 1. Degree derived from fMRI and averaged across all 67 participants of Sample 1. A) Degree during resting state, B) degree during RPM performance, C) difference in degree between RPM performance and resting state.

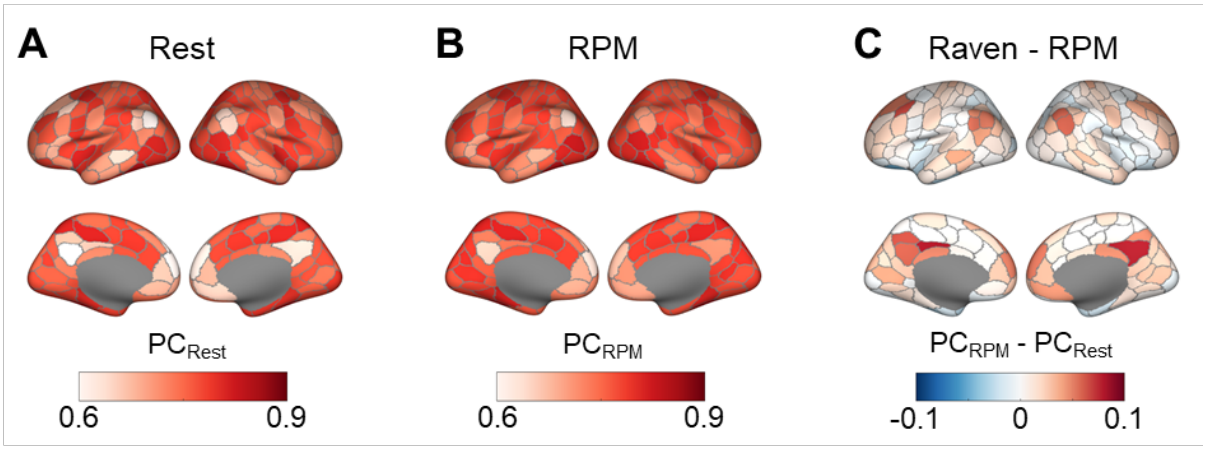

Figure 2. Participation coefficient (PC) derived from fMRI and averaged across all 67 participants of

Sample 1. A) PC during resting state, B) PC during RPM performance, C) difference in PC between RPM performance and resting state.

3.3 EEG-based brain network centrality

EEG-based group-average functional connectivity matrices recorded during resting state and during the RPM task as well as their rest-task difference are illustrated in *Supplement* Figs. S5-S7. Descriptively, resting-state connectivity was highest within the frontal electrode cluster and between frontal and central channels, while no particular weak connections were observed. During RPM performance, this pattern remained the same but was accompanied by a notable decrease in overall connectivity.

Group-average topoplots showing the distribution of degree and participation coefficient for resting state, RPM performance, and their rest-task difference are displayed in Figure 3 and 4. During resting state, both graph measures peaked in frontal and central regions, while during RPM this peak shifted towards frontopolar areas and an additional peak emerged at occipital sides. The topoplot of the difference between resting state and RPM revealed an overall decrease in both connectivity measures, with the decrease being weakest in frontal and occipital regions and highest in right central regions and in a left-lateralized parieto-occipital area.

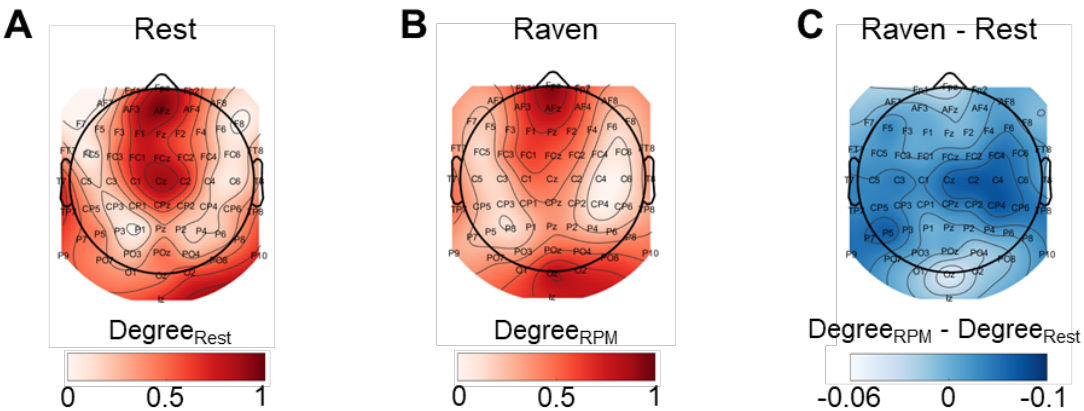

Figure 3. Degree derived from EEG and averaged across the 128 participants of Sample 2. A) Degree during resting state, B) degree during RPM performance, C) difference in degree between RPM

performance and resting state. Note that degree values in A) and B) are normalized to the range [0, 1] for better visualization.

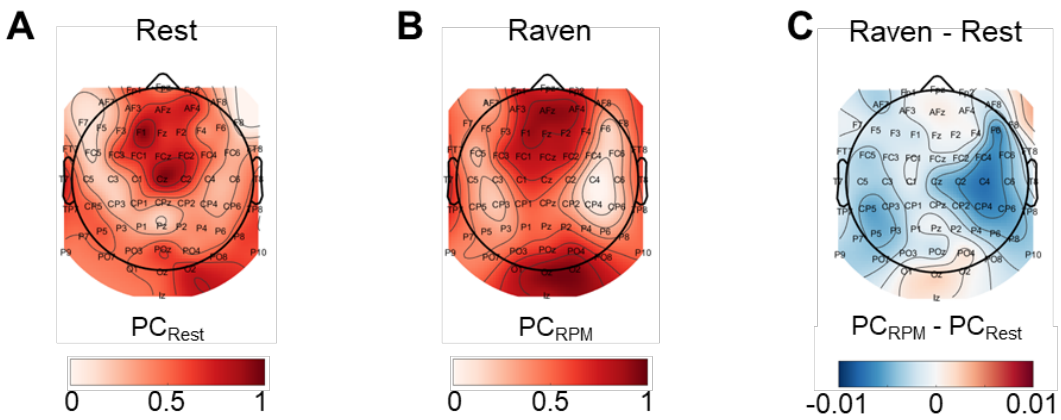

Figure 4. Participation coefficient (PC) derived from EEG and averaged across the 128 participants of Sample 2. A) PC during resting state, B) PC during RPM performance, C) difference in PC between RPM performance and resting state. Note that participation coefficient values in A) and B) are normalized to the range [0, 1] for better visualization.

3.4 Intelligence is associated with fMRI-based connectivity between brain modules

In the fMRI sample, degree demonstrated a trend of mainly positive associations with individual intelligence scores in bilateral somatomotor, left lateral prefrontal and parietal regions as well as in regions of the medial prefrontal cortex (Figure 5, left panel). This trend was strongest in the left dorsolateral prefrontal cortex, in a region of the left ventro-lateral prefrontal cortex, in two regions of the left IPL (one of them belonging to the left TPJ) and in two bilateral somatomotor clusters ($.25 \leq rho \leq .31$, $.013 \leq p \leq .049$, controlled for age, sex, and head motion). However, none of these relationships reached significance when controlling for the number of network nodes for which measures were calculated (200 cortical brain regions). Similar results were observed for varying functional connectivity thresholds (*Supplement* Figs. S8 and S9).

Participation coefficient was positively associated with individual intelligence scores in bilateral and medial prefrontal, bilateral parts of the IPL belonging to the TPJs, and in the posterior cingulate cortex (PCC). A negative association was only observed in one medially located paracentral region (Figure 5). The strongest effects that remained significant even when correcting for the number of network nodes with FDR (200 cortical regions; p(adj) in Figure 5) were observed in a region of the left IPL belonging to the left TPJ (*rho* = .43, $p < .001$, p(adj) = .033), a region of the right IPL belonging to the right TPJ (*rho* = .41, $p < .001$, p(adj) = .039), in the left dorsolateral prefrontal cortex (*rho* = .48, $p < .001$, p(adj) = .013), and in the right dorsolateral prefrontal cortex (*rho* = .42, $p < .001$, p(adj) = .039; note that the latter two associations are only slightly visible in Figure 1 as located along the midline and are therefore highlighted by arrows). Again, similar results could be observed for varying functional connectivity thresholds (*Supplement* Figs. S8 and S9).

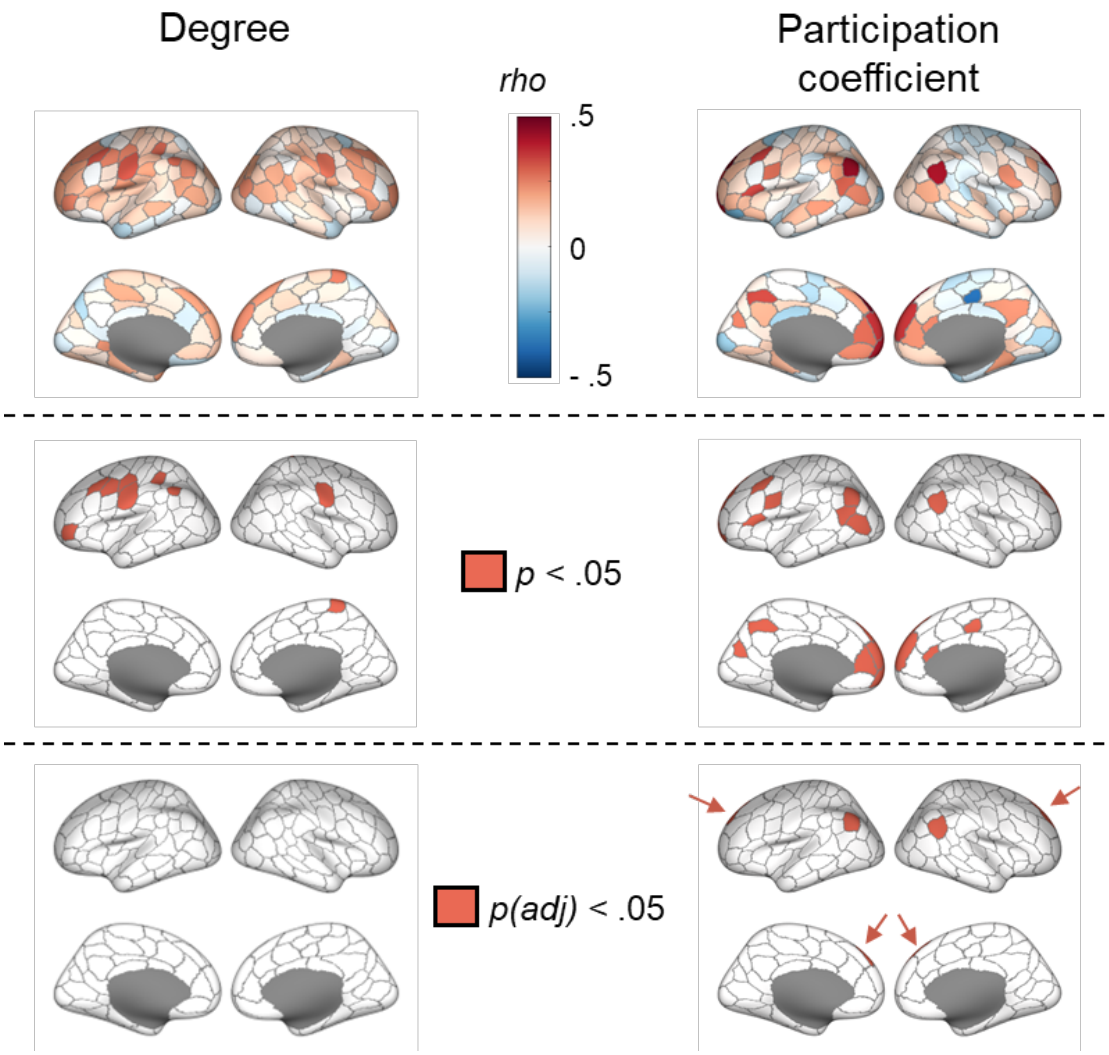

Figure 5. Intelligence is associated with fMRI-based centrality measures during intelligence testing. Associations between individual intelligence scores and variations in degree (left) and participation coefficient (right) in 200 cortical brain regions as assessed with fMRI during performing the RPM. Top panels show the Spearman correlation *rho* controlled for age, sex, and head motion. In center panels, areas with *p*-values < .05, indicating significance (not controlled the number of network nodes, i.e., brain regions) are colored in red (irrespective of whether associations with intelligence were positive or negative). In bottom panels, brain regions with *p*-values < .05 controlled for the number of regions *p*(adj) are colored.

3.5 Complementary insights revealed by EEG

In the EEG sample, the spatial pattern of the relationship between individual variations in degree and individual differences in intelligence varied between different frequencies within the theta band (Figure 6). Averaged across all frequencies of the theta band, higher degree at left frontal and left central electrode positions, as well as along centro-parietal electrodes, was descriptively related to higher intelligence scores, while the degree measured at right central and left parietal electrode positions was negatively associated with intelligence. More specifically, the degree at the left central electrode C1 (*rho* = .18, p = .044, controlled for age, sex, and the number of epochs removed due to artefacts) was positively associated with intelligence, while the degree at the left parietal electrode P3 (*rho* = -.18, p = .039) and at the right central electrode C3 (*rho* = -.30, $p < .001$) were negatively associated. However, these relationships were small to moderate and did not exceed the significance threshold after correcting for the number of channels that served as network nodes (64 electrodes). Similar results were observed for varying functional connectivity thresholds (*Supplement* Figs. S10 and S11).

Also, the spatial pattern of the relationship between the participation coefficient and intelligence varied across different frequencies within the theta band. Averaged across all frequencies of the theta-band, participation coefficient was positively related to intelligence in a frontal cluster including electrodes AF3, F3, F1, Fz, F2, and FCz (Figure 6). Again, correlations were small to moderate ($.19 \leq rho \leq .30$) and not significant after correction for the number of EEG channels (64 electrodes). Note, however, that uncorrected significance ($p < .05$) was observed in six contiguous frontal electrodes, rendering a random nature of this effect unlikely. In the control analyses with different functional connectivity thresholds, the pattern of results was comparable, although the association between participation coefficient and intelligence reached the significance threshold (uncorrected) only for a single electrode of the frontal cluster (FCz) (*Supplement* Figs. S10 and S11).

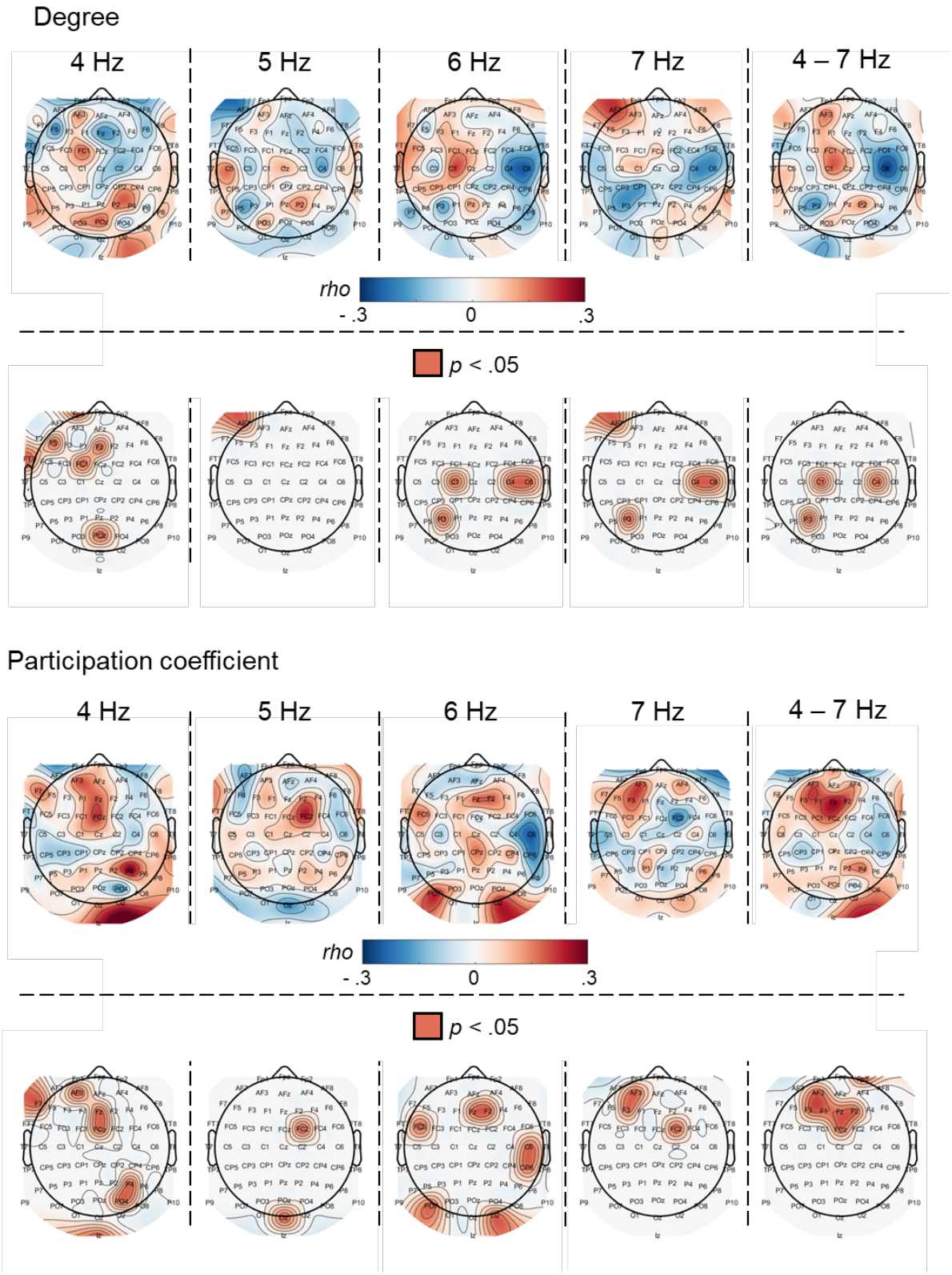

Figure 6. Associations between intelligence and EEG-based centrality measures during intelligence testing. Associations between individual intelligence scores and variations in degree (top) and participation coefficient (bottom) during performing the RPM. The top panels display the Spearman correlation *rho* between intelligence and degree/participation

coefficient assessed at 64 electrodes, controlled for age, sex, and the number of epochs removed due to artefacts. In bottom panels, electrode positions with *p*-values < .05, indicating significance (not controlled for the number of electrodes) are highlighted in red (irrespective of whether associations with intelligence were positive or negative).

Discussion

Our study builds on a large body of research relating individual differences in intelligence to characteristics of functional brain networks, mainly constructed on the basis of fMRI data assessed during resting state or during rather simple cognitive tasks. We extend this research by investigating intelligence-critical connectivity characteristics during behavior actually defining individual differences in intelligence - during performance on a well-established intelligence test. Specifically, we leveraged both fMRI and EEG data to explore how the overall connectedness of brain regions (degree) as well as their participation in intermodular communication (participation coefficient) relates to variations in intelligence. While associations between intelligence and degree did not reach significance, we observed significant associations between individual intelligence scores and intermodular connectedness of specific frontal and parietal brain regions in the fMRI sample. These regions overlap with regions proposed by established intelligence theories (e.g., P-FIT and NNT) and demonstrate the strongest reconfiguration in their connectivity pattern when switching from rest to task. Overall, the observations of this study suggest a critical role of these connector regions in regulating brain activity in diverse functional modules important for solving intelligence tasks successfully.

Intelligence is associated with connectivity between functional brain modules

Although our fMRI results provide trend-level support for previous work that reported links between intelligence and the overall connectedness of brain regions belonging to the

attention- and cognitive control networks (mostly assessed during rest or simple tasks; Hearne et al. 2016; Dubois et al. 2018; Song et al, 2008; Li et al., 2021), the associations observed in our sample did not reach significance when correcting for the number of brain regions (200 nodes). By contrast, relations between intelligence and the intermodular connectedness of brain regions were stronger and significant. This outcome suggests that not simply weaker or stronger connectivity of specific brain regions is critical to intelligent processing but highlights the diversity of connections with which those regions span across different functional brain systems.

Fronto-parietal brain regions as driver of intelligence-critical network states

The brain regions in which we observed significant associations between intelligence and intermodular connectedness comprise two regions of the bilateral dorsolateral prefrontal cortex located along the frontal midline and two parietal regions belonging to the bilateral TPJs. All four regions are included in the brain network responsible for the default mode of human brain functioning (DMN; Raichle et al., 2001) and overlap with regions, whose intrinsic intermodular connectedness has been related to intelligence previously (Hilger et al., 2017) as well as with brain regions proposed as relevant for intelligence differences by the Parieto-Frontal-Integration Theory (P-FIT; Basten et al., 2015; Jung & Haier, 2007) and by subsequent neurocognitive models of intelligence (e.g., multiple-demand theory, Duncan et al., 2010). Interestingly, all significant associations were positive, suggesting that respective fronto-parietal brain regions have more diverse connectivity patterns to other brain modules (beyond the fronto-parietal control network) in people with higher intelligence scores. Thus, while the P-FIT proposes efficient communication *within* the parieto-frontal control network as neural mechanism important to intelligence, the current study extend this proposal in suggesting that increased communication *between* the frontal-parietal network and other networks (*via* prefrontal and parietal hubs) might be key for intelligence-related processing.

Moreover, the same frontal and parietal regions were among those demonstrating the strongest reconfiguration in both centrality measures when switching from rest to task. In general, transition from resting state to task has been found to be accompanied by changes in functional organization from a more modular segregated brain state to a more integrated configuration (Di et al., 2013), i.e., communication between functional networks is increased, especially during cognitive tasks (Cohen & D'Esposito, 2016). The DMN was proposed to play an important role within this process in acting as global integrator, facilitating activity in frontoparietal networks during the conscious processing of information (Dehaene et al., 1998; Guldenmund et al., 2012; Leech et al., 2012; Vatansever et al., 2017; Hearne, 2017). Associations between the success in the intelligence test and the intermodular connectedness of prefrontal and parietal regions of the DMN might therefore be attributed to the role of those regions in increasing the communication between different brain networks and in transitioning into more integrated states, as required for solving complex cognitive tasks such as intelligence tests.

Network flexibility as key mechanism

Based on our findings and previous research, we propose that network flexibility (the ability of brain networks to adapt their connections efficiently to allow for fast switches between cognitive strategies), as a key mechanism of successful intelligence test performance. Although our investigation of brain network characteristics was limited to static connectivity, we hypothesize that specific frontal and parietal brain regions revealed as critical for switches between rest and RPM might also be involved in the dynamic reconfiguration of brain activity states during performing the RPM, reflected in the association between intelligence and intermodular connectedness. This would align with the Network Neuroscience Theory of intelligence, which proposes the flexibility to drive the brain network into different brain

states as a neural foundation of general intelligence (Barbey, 2018) as well as with assumptions that switches in brain activity states are initiated and coordinated by frontoparietal regions through their connections to diverse brain networks (Barbey, 2018; Gu et al., 2015).

More specifically, the Network Neuroscience Theory differentiates between easy and difficult-to-reach brain states in which the brain network transitions to meet specific cognitive demands (Barbey, 2018) Therein, while easy to reach states assumably support crystalized intelligence, difficult-to-reach states are needed for fluid reasoning. Accordingly, an individual's ability to flexibly transition to difficult-to-reach states of brain activity could be considered crucial for succeeding at the Raven's Matrices test, which primarily requires fluid thinking skills and was performed during the recording of brain activity in this study. Interestingly, a relation between individual differences in intelligence and larger changes in functional connectivity to rare distant brain activity states during cognition, potentially reflecting such difficult-to-reach states, has recently been demonstrated in a study using dynamic network analyses (Ng et al., 2024). Further, it has been suggested that efficient intermodular connectedness is required to initiate these changes into difficult-to-reach states and might be coordinated by specific brain regions (Cole 2013). Our study suggests that prefrontal and parietal brain regions, in particular the dorsolateral prefrontal near the frontal midline and the IPL part of the TPJ, might be critically involved in this coordination process, i.e., for transitioning the brain flexibly into required brain states including difficult-to-reach states. This proposal requires further investigation and presents a promising avenue for future studies combining graph theory with measures from network control theory.

Complementary insights from EEG

Our results reveal a tendency of higher theta-band connectivity in frontal brain regions during intelligence test performance related to higher intelligence scores. Although, effect sizes were small to moderate and did not reach significance, the pattern of this trend corroborates our proposal as well as previous EEG studies suggesting theta-band neural activity to reflect cognitively relevant long-range processing (Cohen, 2011; Schubert, 2021), orchestrated by prefrontal regions (Helfrich & Knight, 2016). However, given the small to moderate effects, future studies utilizing larger samples, best in combination with a larger trial number (und thus higher statistical power; Nebe et al. 2013) should aim for replication. Also, it remains unclear, if EEG theta band connectivity reflects similar properties of neural long-range processing as fMRI connectivity or if both methods may capture independent neural aspects. In this regard, future studies simultaneously assessing fMRI and EEG during intelligence testing (Hilger et al. 2022) or using magnetoencephalography (MEG; Bruzzone et al., 2022) are imperative.

Limitations and future directions

Our study has limitations. First, our sample sizes were limited, critically diminishing the statistical power to detect small effects (Nebe et al., 2023; DeYoung et al., 2022, 2024; Marek et al., 2022). Also, we had no access to a sample in which we could test for independent replication. Therefore, results should be interpreted with caution and future studies with larger samples (and higher numbers of trials) are essentially required to study this subject with larger power. Second, fMRI and EEG data stem from different samples, preventing direct comparisons. Although, our study is the first combining both complementary methods to study this research question at all, future studies should employ methods of high spatial and high temporal resolution in the same participants (e.g., using MEG). Third, all analyses were based on time-averaged connectivity that allow only indirect insights into neural dynamics. Dynamic connectivity analyses (Esfalani et al., 2018; Wehrheim et al., 2023) may therefore

present a further promising route but would require longer trials and a better temporal resolution in fMRI recordings. Fourth, the age range of both samples was restricted to young adults. Thus, a last suggestion to future study is the investigation of older and especially younger participants, as the latter, best combined with the analysis of structural brain networks, may inform about hypotheses whether the higher diversity of intermodular connections observed in fronto-parietal brain regions may present an innate attribute or reflect previous experience.

Conclusion

Our study reveals that the diversity with which specific fronto-parietal brain regions connect to different brain modules is significantly associated with individuals' performance on an established intelligence test. These brain regions show strong reconfiguration in their functional connectivity when switching from rest to task and might be involved in coordinating the communication between brain networks in adaptation to increasing task demands, thus facilitating successful task performance. Overall, this study demonstrates the value of investigating the neural underpinnings of individual differences in intelligence during intelligence test performance and should motivate researchers to explore different methodologies of brain activity assessment towards this goal.

Acknowledgements

This work was supported by the German Research Foundation (DFG, grant HI 2185/1-3 to K.H.), by the Heinrich-Böll Foundation (funds from the Federal Ministry of Education and Research, grant P145957 to J.A.T.), and by the Open Access Publication Fund of the University of Würzburg. Further, this research was supported in part by Lilly Endowment, Inc., through its support for the Indiana University Pervasive Technology Institute. This research was supported by a grant from the John Templeton Foundation (Grant # 22156)

entitled “The Neuroscience of Scientific Creativity.” A.Ch. was supported by grant #2019/33/B/HS6/00321 from the National Science Centre of Poland.

Author contributions

J.A.T.: Conceptualization, methodology, software, formal analysis, data curation, visualization, writing—original draft, funding acquisition. J.F.: Methodology, software, data curation, writing—review & editing. O.S.: Methodology, writing—review & editing. A.C.: Investigation, writing—review & editing. R.J.: Investigation, writing—review & editing. K.H.: Conceptualization, methodology, writing—original draft, supervision, project administration, funding acquisition.

References

Abraham, A., Pedregosa, F., Eickenberg, M., Gervais, P., Mueller, A., Kossaifi, J., Gramfort, A., Thirion, B., & Varoquaux, G. (2014). Machine learning for neuroimaging with scikit-learn. *Frontiers in Neuroinformatics*, *8*, 71792. https://doi.org/10.3389/fninf.2014.00014

Anderson, E. D., & Barbey, A. K. (2023). Investigating cognitive neuroscience theories of human intelligence: A connectome-based predictive modeling approach. *Human Brain Mapping*, *44*(4), 1647–1665. https://doi.org/10.1002/hbm.26164

Avants, B., Epstein, C., Grossman, M., & Gee, J. (2008). Symmetric diffeomorphic image registration with cross-correlation: Evaluating automated labeling of elderly and neurodegenerative brain. *Medical Image Analysis*, *12*(1), 26–41. https://doi.org/10.1016/j.media.2007.06.004

Barbey, A. K. (2018). Network Neuroscience Theory of Human Intelligence. *Trends in Cognitive Sciences*, *22*(1), 8–20. https://doi.org/10.1016/j.tics.2017.10.001

Basten, U., Hilger, K., & Fiebach, C. J. (2015). Where smart brains are different: A quantitative meta-analysis of functional and structural brain imaging studies on intelligence. *Intelligence, 51*, 10-27.

Behzadi, Y., Restom, K., Liau, J., & Liu, T. T. (2007). A component based noise correction method (CompCor) for BOLD and perfusion based fMRI. *NeuroImage*, *37*(1), 90–101. https://doi.org/10.1016/j.neuroimage.2007.04.042

Ben-Shachar, M. S. (2018). TBT: Reject and Interpolate channels on a trial-by-trial basis. Zenodo. https://doi.org/10.5281/zenodo.1241518

Blondel, V. D., Guillaume, J.-L., Lambiotte, R., & Lefebvre, E. (2008). Fast unfolding of communities in large networks. *Journal of Statistical Mechanics: Theory and Experiment*, *2008*(10), P10008. https://doi.org/10.1088/1742-5468/2008/10/P10008

Braun, U., Schäfer, A., Walter, H., Erk, S., Romanczuk-Seiferth, N., Haddad, L., Schweiger, J. I., Grimm, O., Heinz, A., Tost, H., Meyer-Lindenberg, A., & Bassett, D. S. (2015). Dynamic reconfiguration of frontal brain networks during executive cognition in humans. *Proceedings of the National Academy of Sciences*, *112*(37), 11678–11683. https://doi.org/10.1073/pnas.1422487112

Bruzzone, S. E. P., Lumaca, M., Brattico, E., Vuust, P., Kringelbach, M. L., & Bonetti, L. (2022). Dissociated brain functional connectivity of fast versus slow frequencies underlying individual differences in fluid intelligence: a DTI and MEG study. *Scientific Reports*, *12*(1), 4746. https://doi.org/10.1038/s41598-022-08521-5

Calvin, C. M., Deary, I. J., Fenton, C., Roberts, B. A., Der, G., Leckenby, N., & Batty, G. D. (2011). Intelligence in youth and all-cause-mortality: systematic review with meta-analysis. International journal of epidemiology, 40(3), 626-644.

Chuderski, A. (2016). Fluid Intelligence and the Cross-Frequency Coupling of Neuronal Oscillations. *The Spanish Journal of Psychology*, *19*, E91. https://doi.org/10.1017/SJP.2016.86

Cohen, J. R., & D'Esposito, M. (2016). The segregation and integration of distinct brain networks and their relationship to cognition. *Journal of Neuroscience*, *36*(48), 12083–12094. https://doi.org/10.1523/JNEUROSCI.2965-15.2016

Cohen, M. X. (2011). Error-related medial frontal theta activity predicts cingulate-related structural connectivity. *NeuroImage*, *55*(3), 1373–1383. https://doi.org/10.1016/j.neuroimage.2010.12.072

Cole, M. W., Ito, T., & Braver, T. S. (2015). Lateral prefrontal cortex contributes to fluid intelligence through multinetwork connectivity. *Brain Connectivity*, *5*(8), 497–504. https://doi.org/10.1089/brain.2015.0357

Cole, M. W., Reynolds, J. R., Power, J. D., Repovs, G., Anticevic, A., & Braver, T. S. (2013). Multi-task connectivity reveals flexible hubs for adaptive task control. *Nature Neuroscience*, *16*(9), 1348–1355. https://doi.org/10.1038/nn.3470

Cole, M. W., Ito, T., Schultz, D., Mill, R., Chen, R., & Cocuzza, C. (2019). Task activations produce spurious but systematic inflation of task functional connectivity estimates. *NeuroImage*, *189*, 1–18. https://doi.org/10.1016/j.neuroimage.2018.12.054

Cox, R. W., & Hyde, J. S. (1997). Software tools for analysis and visualization of fMRI data. *NMR in Biomedicine*, *10*(4–5), 171–178. https://doi.org/10.1002/(SICI)1099-1492(199706/08)10:4/5<171::AID-NBM453>3.0.CO;2-L

Dale, A. M., Fischl, B., & Sereno, M. I. (1999). Cortical Surface-Based Analysis. *NeuroImage*, *9*(2), 179–194. https://doi.org/10.1006/nimg.1998.0395

Deary, I. J. (2012). Intelligence. *Annual Review of Psychology*, *63*, 453–482.

Dehaene, S., Kerszberg, M., & Changeux, J.-P. (1998). A neuronal model of a global workspace in effortful cognitive tasks. *Proceedings of the National Academy of Sciences*, *95*(24), 14529–14534. https://doi.org/10.1073/pnas.95.24.14529

Delorme, A., & Makeig, S. (2004). EEGLAB: an open source toolbox for analysis of single-trial EEG dynamics including independent component analysis. *Journal of Neuroscience Methods*, *134*(1), 9–21. https://doi.org/10.1016/j.jneumeth.2003.10.009

DeYoung, C. G., Sassenberg, T., Abend, R., Allen, T., Beaty, R., Bellgrove, M., … Wacker, J. (2022). Reproducible between-person brain-behavior associations do not always require thousands of individuals. https://doi.org/10.31234/osf.io/sfnmk

DeYoung, C. G., Hilger, K., Hanson, J. L., Abend, R., Allen, T., Beaty, R., Blain, S. D., Chavez, R. S., Engel, S. A., Ma, F., Fornito, A., Genç, E., Goghari, V., Grazioplene, R. G., Homan, P., Joyner, K., Kaczkurkin, A. N., Latzman, R. D., Martin, E. A., … Wacker, J. (in press). Beyond increasing sample sizes: Optimizing effect sizes in neuroimaging research on individual differences. *Journal of Cognitive Neuroscience.*

Di, X., Gohel, S., Kim, E. H., & Biswal, B. B. (2013). Task vs. rest—different network configurations between the coactivation and the resting-state brain networks. *Frontiers in Human Neuroscience*, *7*. https://doi.org/10.3389/fnhum.2013.00493

Dubois, J., Galdi, P., Paul, L. K., & Adolphs, R. (2018). A distributed brain network predicts general intelligence from resting-state human neuroimaging data.

Philosophical Transactions of the Royal Society B: Biological Sciences, *373*(1756), 20170284. https://doi.org/10.1098/rstb.2017.0284

Duncan, J. (2010). The multiple-demand (MD) system of the primate brain: mental programs for intelligent behaviour. *Trends in Cognitive Sciences*, *14*(4), 172–179. https://doi.org/10.1016/j.tics.2010.01.004

Ebisch, S. J., Perrucci, M. G., Mercuri, P., Romanelli, R., Mantini, D., Romani, G. L., Colom, R., & Saggino, A. (2012). Common and unique neuro-functional basis of induction, visualization, and spatial relationships as cognitive components of fluid intelligence. *NeuroImage*, *62*(1), 331–342. https://doi.org/10.1016/j.neuroimage.2012.04.053

Esteban, O., Blair, R., Markiewicz, Christopher J. Berleant, Shoshana L. Moodie, C., Ma, F., Isik, A. I., Erramuzpe, A., Kent, J. D., Goncalves, M., DuPre, E., Sitek, K. R., Gomez, D. E. P., Lurie, D. J., Ye, Z., & Poldrack, Russell A. Gorgolewski, K. J. (2018). fMRIPrep 22.0.0. *Software*. https://doi.org/10.5281/zenodo.852659

Esteban, O., Markiewicz, C. J., Blair, R. W., Moodie, C. A., Isik, A. I., Erramuzpe, A., Kent, J. D., Goncalves, M., DuPre, E., Snyder, M., Oya, H., Ghosh, S. S., Wright, J., Durnez, J., Poldrack, R. A., & Gorgolewski, K. J. (2019). fMRIPrep: a robust preprocessing pipeline for functional MRI. *Nature Methods*, *16*(1), 111–116. https://doi.org/10.1038/s41592-018-0235-4

Ferguson, M. A., Anderson, J. S., & Spreng, R. N. (2017). Fluid and flexible minds: Intelligence reflects synchrony in the brain's intrinsic network architecture. *Network Neuroscience*, *1*(2), 192–207. https://doi.org/10.1162/netn_a_00010

Fonov, V., Evans, A., McKinstry, R., Almli, C., & Collins, D. (2009). Unbiased nonlinear average age-appropriate brain templates from birth to adulthood. *NeuroImage*, *47*, S102. https://doi.org/10.1016/S1053-8119(09)70884-5

Gągol, A., Magnuski, M., Kroczek, B., Kałamała, P., Ociepka, M., Santarnecchi, E., & Chuderski, A. (2018). Delta-gamma coupling as a potential neurophysiological mechanism of fluid intelligence. *Intelligence*, *66*, 54–63. https://doi.org/10.1016/j.intell.2017.11.003

Galton, F. (1883). Inquiries into Human Faculty and Its Development. Dent.

Gil Ávila, C., Bott, F. S., Tiemann, L., Hohn, V. D., May, E. S., Nickel, M. M., Zebhauser, P. T., Gross, J., & Ploner, M. (2023). DISCOVER-EEG: an open, fully automated EEG pipeline for biomarker discovery in clinical neuroscience. *Scientific Data*, *10*(1), 613. https://doi.org/10.1038/s41597-023-02525-0

Girn, M., Mills, C., & Christoff, K. (2019). Linking brain network reconfiguration and intelligence: Are we there yet? *Trends in Neuroscience and Education*, *15*, 62–70. https://doi.org/10.1016/j.tine.2019.04.001

Gomez-Herrero, G., De Clercq, W., Anwar, H., Kara, O., Egiazarian, K., Van Huffel, S., & Van Paesschen, W. (2006). Automatic Removal of Ocular Artifacts in the EEG without an EOG Reference Channel. *Proceedings of the 7th Nordic Signal Processing Symposium - NORSIG 2006*, 130–133. https://doi.org/10.1109/NORSIG.2006.275210

Gorgolewski, K. J., Burns, C. D., Madison, C., Clark, D., Halchenko, Y. O., Waskom, M. L., & Ghosh, S. S. (2011). Nipype: A Flexible, Lightweight and Extensible Neuroimaging Data Processing Framework in Python. *Frontiers in Neuroinformatics*, *5*, 13. https://doi.org/10.3389/fninf.2011.00013

Gorgolewski, K. J., Esteban, O., Markiewicz, C. J., Ziegler, E., Ellis, D. G., Notter, M. P., Jarecka, D., Johnson, H., Burns, C., Manhães-Savio, A., Hamalainen, C., Yvernault, B., Salo, T., Jordan, K., Goncalves, M., Waskom, M., Clark, D., Wong, J., Loney, F., … Ghosh, S. (2018). Nipype. *Software*. https://doi.org/10.5281/zenodo.596855

Greene, A. S., Gao, S., Noble, S., Scheinost, D., & Constable, R. T. (2020). How Tasks Change Whole-Brain Functional Organization to Reveal Brain-Phenotype Relationships. *Cell Reports*, *32*(8), 108066. https://doi.org/10.1016/j.celrep.2020.108066

Greve, D. N., & Fischl, B. (2009). Accurate and robust brain image alignment using boundary-based registration. *NeuroImage*, *48*(1), 63–72. https://doi.org/10.1016/j.neuroimage.2009.06.060

Gu, S., Pasqualetti, F., Cieslak, M., Telesford, Q. K., Yu, A. B., Kahn, A. E., Medaglia, J. D., Vettel, J. M., Miller, M. B., Grafton, S. T., & Bassett, D. S. (2015). Controllability of structural brain networks. *Nature Communications*, *6*(1), 8414. https://doi.org/10.1038/ncomms9414

Guimerà, R., & Nunes Amaral, L. A. (2005). Functional cartography of complex metabolic networks. *Nature*, *433*(7028), 895–900. https://doi.org/10.1038/nature03288

Guldenmund, P., Vanhaudenhuyse, A., Boly, M., Laureys, S., & Soddu, A. (2012). A default mode of brain function in altered states of consciousness. *Archives italiennes de biologie*, *150*(2/3), 107-121.

Haier, R. J. (2017). *The neuroscience of intelligence*. Cambridge University Press. https://doi.org/10.1017/9781316105771

He, P., Wilson, G., & Russell, C. (2004). Removal of ocular artifacts from electro-encephalogram by adaptive filtering. *Medical & Biological Engineering & Computing*, *42*(3), 407–412. https://doi.org/10.1007/BF02344717

Hearne, L. J., Cocchi, L., Zalesky, A., & Mattingley, J. B. (2017). Reconfiguration of Brain Network Architectures between Resting-State and Complexity-Dependent Cognitive Reasoning. *The Journal of Neuroscience*, *37*(35), 8399–8411. https://doi.org/10.1523/JNEUROSCI.0485-17.2017

Hearne, L. J., Mattingley, J. B., & Cocchi, L. (2016). Functional brain networks related to individual differences in human intelligence at rest. *Scientific Reports*, *6*(1), 32328. https://doi.org/10.1038/srep32328

Helfrich, R. F., & Knight, R. T. (2016). Oscillatory Dynamics of Prefrontal Cognitive Control. *Trends in Cognitive Sciences*, *20*(12), 916–930. https://doi.org/10.1016/j.tics.2016.09.007

Hilger, K., Ekman, M., Fiebach, C. J., & Basten, U. (2017). Efficient hubs in the intelligent brain: Nodal efficiency of hub regions in the salience network is associated with general intelligence. *Intelligence*, *60*, 10–25. https://doi.org/10.1016/j.intell.2016.11.001

Hilger, K., Fukushima, M., Sporns, O., & Fiebach, C. J. (2020). Temporal stability of functional brain modules associated with human intelligence. *Human Brain Mapping*, *41*(2), 362–372. https://doi.org/10.1002/hbm.24807

Hilger, K., Spinath, F. M., Troche, S., & Schubert, A.-L. (2022). The biological basis of intelligence: Benchmark findings. *Intelligence*, *93*, 101665. https://doi.org/10.1016/j.intell.2022.101665

Hilger, K., & Sporns, O. (2021). Network neuroscience methods for studying intelligence. In A. K. Barbey, K. Sherif, & R. J. Haier (Eds.), *The Cambridge handbook of intelligence and cognitive neuroscience* (pp. 26–43). Cambridge University Press. https://doi.org/10.1017/9781108635462.004

Jenkinson, M., Bannister, P., Brady, M., & Smith, S. (2002). Improved Optimization for the Robust and Accurate Linear Registration and Motion Correction of Brain Images. *NeuroImage*, *17*(2), 825–841. https://doi.org/10.1006/nimg.2002.1132

Jung, R. E., & Haier, R. J. (2007). The Parieto-Frontal Integration Theory (P-FIT) of intelligence: Converging neuroimaging evidence. *Behavioral and Brain Sciences*, *30*(2), 135–154. https://doi.org/10.1017/S0140525X07001185

Klein, A., Ghosh, S. S., Bao, F. S., Giard, J., Häme, Y., Stavsky, E., Lee, N., Rossa, B., Reuter, M., Chaibub Neto, E., & Keshavan, A. (2017). Mindboggling morphometry of human brains. *PLOS Computational Biology*, *13*(2), e1005350. https://doi.org/10.1371/journal.pcbi.1005350

Langer, N., Pedroni, A., Gianotti, L. R. R., Hänggi, J., Knoch, D., & Jäncke, L. (2012). Functional brain network efficiency predicts intelligence. *Human Brain Mapping*, *33*(6), 1393–1406. https://doi.org/10.1002/hbm.21297

Lee, K. H., Choi, Y. Y., Gray, J. R., Cho, S. H., Chae, J.-H., Lee, S., & Kim, K. (2006). Neural correlates of superior intelligence: Stronger recruitment of posterior parietal cortex. *NeuroImage*, *29*(2), 578–586. https://doi.org/10.1016/j.neuroimage.2005.07.036

Leech, R., Braga, R., & Sharp, D. J. (2012). Echoes of the Brain within the Posterior Cingulate Cortex. *The Journal of Neuroscience*, *32*(1), 215–222. https://doi.org/10.1523/JNEUROSCI.3689-11.2012

Li, Y., Xue, Y.-Z., Zhao, W.-T., Li, S.-S., Li, J., & Xu, Y. (2021). Correlates of intelligence via resting-state functional connectivity of the amygdala in healthy adults. *Brain Research*, *1751*, 147176. https://doi.org/10.1016/j.brainres.2020.147176

Marek, S., Tervo-Clemmens, B., Calabro, F. J., Montez, D. F., Kay, B. P., Hatoum, A. S., Donohue, M. R., Foran, W., Miller, R. L., Hendrickson, T. J., Malone, S. M., Kandala, S., Feczko, E., Miranda-Dominguez, O., Graham, A. M., Earl, E. A., Perrone, A. J., Cordova, M., Doyle, O., … Dosenbach, N. U. F. (2022). Reproducible brain-wide association studies require thousands of individuals. *Nature*, *603*(7902), 654–660. https://doi.org/10.1038/s41586-022-04492-9

Muschelli, J., Nebel, M. B., Caffo, B. S., Barber, A. D., Pekar, J. J., & Mostofsky, S. H. (2014). Reduction of motion-related artifacts in resting state fMRI using aCompCor. *NeuroImage*, *96*, 22–35. https://doi.org/10.1016/j.neuroimage.2014.03.028

Nebe, S., Reutter, M., Baker, D. H., Bölte, J., Domes, G., Gamer, M., ... & Feld, G. B. (2023). Enhancing precision in human neuroscience. Elife, 12, e85980.

Ng, J., Yu, J.-C., Feusner, J. D., & Hawco, C. (2024). Higher general intelligence is associated with stable, efficient, and typical dynamic functional brain connectivity patterns. *Imaging Neuroscience*, *2*, 1–34. https://doi.org/10.1162/imag_a_00234

Ociepka, M., Kałamała, P., & Chuderski, A. (2023). Take your time: Slow brain rhythms predict fluid intelligence. *Intelligence*, *100*, 101780. https://doi.org/10.1016/j.intell.2023.101780

Oostenveld, R., Fries, P., Maris, E., & Schoffelen, J.-M. (2011). FieldTrip: Open Source Software for Advanced Analysis of MEG, EEG, and Invasive

Electrophysiological Data. *Computational Intelligence and Neuroscience*, *2011*, 1–9. https://doi.org/10.1155/2011/156869

Pahor, A., & Jaušovec, N. (2014). Theta–gamma cross-frequency coupling relates to the level of human intelligence. *Intelligence, 46*, 283-290.

Parkes, L., Fulcher, B., Yücel, M., & Fornito, A. (2018). An evaluation of the efficacy, reliability, and sensitivity of motion correction strategies for resting-state functional MRI. *NeuroImage*, *171*, 415–436. https://doi.org/10.1016/j.neuroimage.2017.12.073

Perfetti, B., Saggino, A., Ferretti, A., Caulo, M., Romani, G. L., & Onofrj, M. (2009). Differential patterns of cortical activation as a function of fluid reasoning complexity. *Human Brain Mapping*, *30*(2), 497–510. https://doi.org/10.1002/hbm.20519

Power, J. D., Mitra, A., Laumann, T. O., Snyder, A. Z., Schlaggar, B. L., & Petersen, S. E. (2014). Methods to detect, characterize, and remove motion artifact in resting state fMRI. *NeuroImage*, *84*, 320–341. https://doi.org/10.1016/j.neuroimage.2013.08.048

Power, J. D., Schlaggar, B. L., Lessov-Schlaggar, C. N., & Petersen, S. E. (2013). Evidence for hubs in human functional brain networks. *Neuron*, *79*(4), 798–813. https://doi.org/10.1016/j.neuron.2013.07.035

Raichle, M. E., MacLeod, A. M., Snyder, A. Z., Powers, W. J., Gusnard, D. A., & Shulman, G. L. (2001). A default mode of brain function. *Proceedings of the National Academy of Sciences*, *98*(2), 676–682. https://doi.org/10.1073/pnas.98.2.676

Raven, J. C. (1990). *Advanced Progressive Matrices: Sets I and II*. Oxford University Press.

Raven, J. C., Raven, J., & Court, J. H. (1998). *Manual for Raven's progressive matrices and vocabulary scales*. Oxford Psychologists Press.

Reichardt, J., & Bornholdt, S. (2006). Statistical mechanics of community detection. *Physical Review E*, *74*(1), 016110. https://doi.org/10.1103/PhysRevE.74.016110

Ronhovde, P., & Nussinov, Z. (2009). Multiresolution community detection for megascale networks by information-based replica correlations. *Physical Review E*, *80*(1), 016109. https://doi.org/10.1103/PhysRevE.80.016109

Rubinov, M., & Sporns, O. (2010). Complex network measures of brain connectivity: Uses and interpretations. *NeuroImage*, *52*(3), 1059–1069. https://doi.org/10.1016/j.neuroimage.2009.10.003

Rubinov, M., & Sporns, O. (2011). Weight-conserving characterization of complex functional brain networks. *NeuroImage*, *56*(4), 2068–2079. https://doi.org/10.1016/j.neuroimage.2011.03.069

Safron, A., Klimaj, V., & Hipólito, I. (2022). On the importance of being flexible: dynamic brain networks and their potential functional significances. Frontiers in Systems Neuroscience, 15, 688424.

Sassenberg, T. A., Safron, A., & DeYoung, C. G. (2024). Stable individual differences from dynamic patterns of function: brain network flexibility predicts openness/intellect, intelligence, and psychoticism. Cerebral Cortex, 34(9), bhae391.

Saxe, G. N., Calderone, D., & Morales, L. J. (2018). Brain entropy and human intelligence: A resting-state fMRI study. PloS one, 13(2), e0191582.

Schubert, A.-L., Hagemann, D., Löffler, C., Rummel, J., & Arnau, S. (2021). A chronometric model of the relationship between frontal midline theta functional connectivity and human intelligence. *Journal of Experimental Psychology: General*, *150*(1), 1–22. https://doi.org/10.1037/xge0000865

Schultz, D. H., & Cole, M. W. (2016). Higher intelligence is associated with less task-related brain network reconfiguration. *Journal of Neuroscience*, *36*(33), 8551–8561. https://doi.org/10.1523/JNEUROSCI.0358-16.2016

Shine, J. M., Breakspear, M., Bell, P. T., Ehgoetz Martens, K. A., Shine, R., Koyejo, O., Sporns, O., & Poldrack, R. A. (2019). Human cognition involves the dynamic integration of neural activity and neuromodulatory systems. *Nature Neuroscience*, *22*(2), 289–296. https://doi.org/10.1038/s41593-018-0312-0

Song, M., Zhou, Y., Li, J., Liu, Y., Tian, L., Yu, C., & Jiang, T. (2008). Brain spontaneous functional connectivity and intelligence. *NeuroImage*, *41*(3), 1168–1176. https://doi.org/10.1016/j.neuroimage.2008.02.036

Soreq, E., Violante, I. R., Daws, R. E., & Hampshire, A. (2021). Neuroimaging evidence for a network sampling theory of individual differences in human intelligence test performance. *Nature Communications*, *12*(1), 2072. https://doi.org/10.1038/s41467-021-22199-9

Spearman, C. (1904). "General intelligence," objectively determined and measured. *The American Journal of Psychology*, *15*(2), 201–292. https://doi.org/10.2307/141210

Sripada, C., Angstadt, M., Rutherford, S., Taxali, A., & Shedden, K. (2020). Toward a "treadmill test" for cognition: Improved prediction of general cognitive ability from the

task activated brain. *Human Brain Mapping*, *41*(12), 3186–3197. https://doi.org/10.1002/hbm.25007

Sternberg, R. J. (1997). The concept of intelligence and its role in lifelong learning and success. American psychologist, 52(10), 1030.

Sun, Y., Danila, B., Josić, K., & Bassler, K. E. (2009). Improved community structure detection using a modified fine-tuning strategy. *EPL (Europhysics Letters)*, *86*(2), 28004. https://doi.org/10.1209/0295-5075/86/28004

Thiele, J. A., Faskowitz, J., Sporns, O., & Hilger, K. (2022). Multitask brain network reconfiguration is inversely associated with human intelligence. *Cerebral Cortex*, *32*(19), 4172–4182. https://doi.org/10.1093/cercor/bhab473

Thiele, J. A., Faskowitz, J., Sporns, O., & Hilger, K. (2024). Choosing explanation over performance: Insights from machine learning-based prediction of human intelligence from brain connectivity. *PNAS Nexus*, *3*(12). https://doi.org/10.1093/pnasnexus/pgae519

Tustison, N. J., Avants, B. B., Cook, P. A., Yuanjie Zheng, Egan, A., Yushkevich, P. A., & Gee, J. C. (2010). N4ITK: Improved N3 Bias Correction. *IEEE Transactions on Medical Imaging*, *29*(6), 1310–1320. https://doi.org/10.1109/TMI.2010.2046908

Vakhtin, A. A., Ryman, S. G., Flores, R. A., & Jung, R. E. (2014). Functional brain networks contributing to the Parieto-Frontal Integration Theory of Intelligence. *NeuroImage*, *103*, 349–354. https://doi.org/10.1016/j.neuroimage.2014.09.055

Vatansever, D., Manktelow, A. E., Sahakian, B. J., Menon, D. K., & Stamatakis, E. A. (2017). Angular default mode network connectivity across working memory load. *Human Brain Mapping*, *38*(1), 41–52. https://doi.org/10.1002/hbm.23341

Yeo, T. B. T., Krienen, F. M., Sepulcre, J., Sabuncu, M. R., Lashkari, D., Hollinshead, M., Roffman, J. L., Smoller, J. W., Zöllei, L., Polimeni, J. R., Fischl, B., Liu, H., & Buckner, R. L. (2011). The organization of the human cerebral cortex estimated by intrinsic functional connectivity. *Journal of Neurophysiology*, *106*(3), 1125–1165. https://doi.org/10.1152/jn.00338.2011

Zhang, Y., Brady, M., & Smith, S. (2001). Segmentation of brain MR images through a hidden Markov random field model and the expectation-maximization algorithm. *IEEE Transactions on Medical Imaging*, *20*(1), 45–57. https://doi.org/10.1109/42.906424

Zurrin, R., Wong, S. T. S., Roes, M. M., Percival, C. M., Chinchani, A., Arreaza, L., Kusi, M., Momeni, A., Rasheed, M., Mo, Z., Goghari, V. M., & Woodward, T. S. (2024). Functional brain networks involved in the Raven's standard progressive matrices task and their relation to theories of fluid intelligence. *Intelligence*, *103*, 101807. https://doi.org/10.1016/j.intell.2024.101807

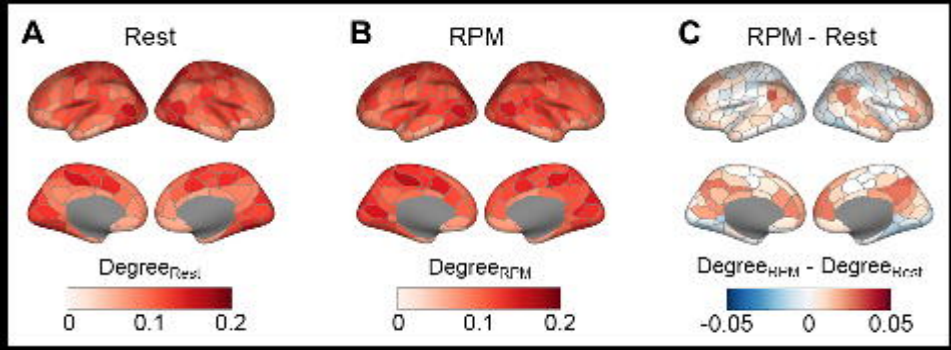
A
Rest
B
RPM
C
RPM - Rest
Degree$_{Rest}$
0
0.1
0.2
Degree$_{RPM}$
0
0.1
0.2
Degree$_{RPM}$ - Degree$_{Rest}$
-0.05
0
0.05

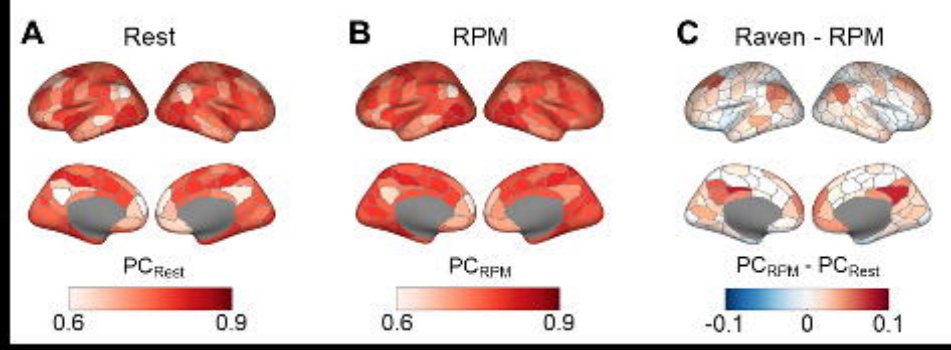
A
Rest
PC_Rest
0.6
0.9
B
RPM
PC_RPM
0.6
0.9
C
Raven - RPM
PC_RPM - PC_Rest
-0.1
0
0.1

Rest
Degree$_{Rest}$
Raven
Degree$_{RPM}$
Raven - Rest
gree$_{RPM}$ - Degree$_{RA}$

Rest
PC_Rest

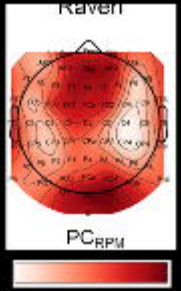
Raven
PC_RPM

Raven - Rest
PC_RPM - PC_Rest

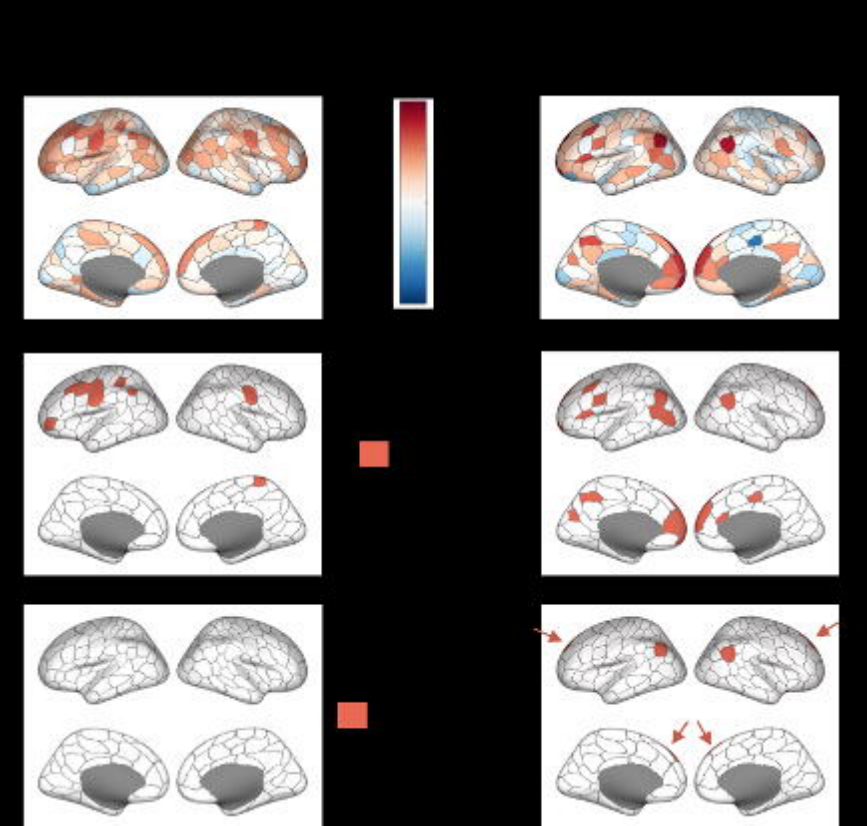

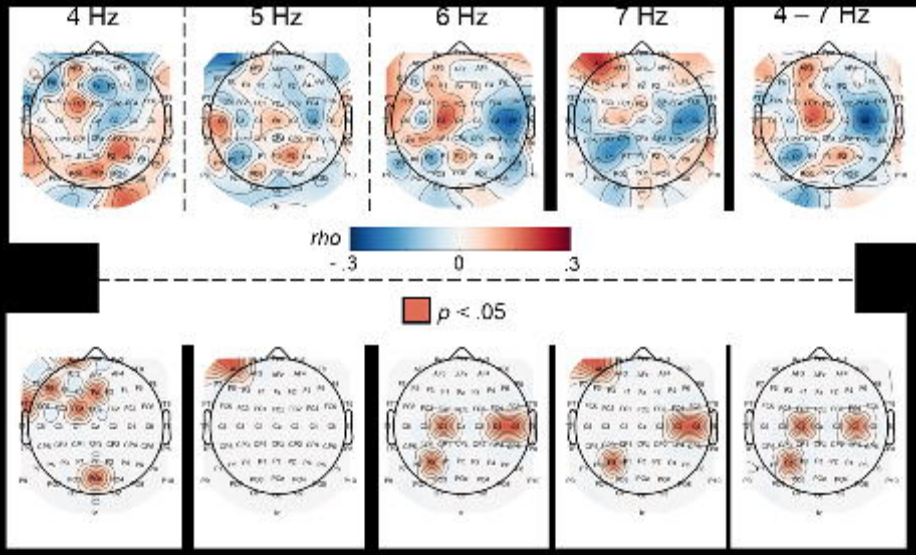
4 Hz
5 Hz
6 Hz
7 Hz
4 – 7 Hz
rho
- .3
0
.3
p < .05

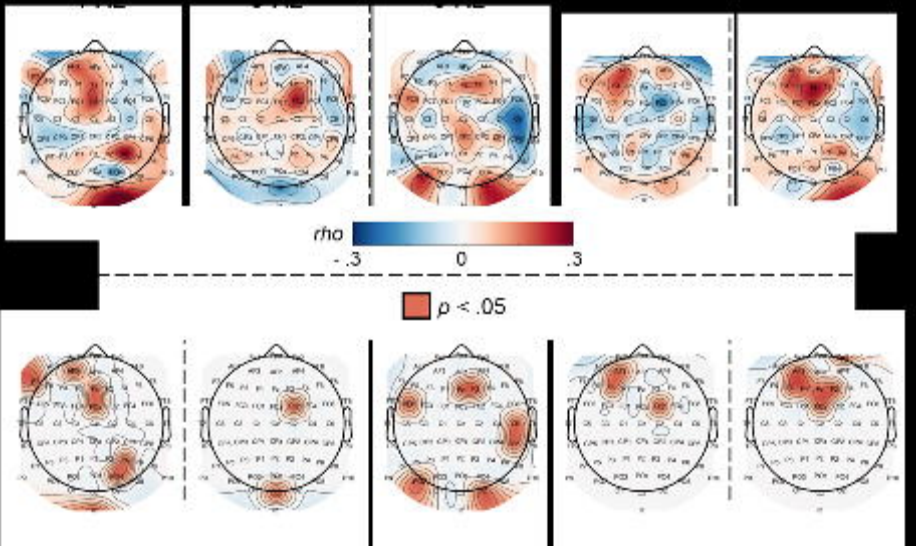
rho
- .3
0
.3
p < .05